Cancer Chemother Pharmacol (2009) 63:191–200
DOI 10.1007/s00280-008-0726-6

ORIGINAL ARTICLE

cis-3, 4′, 5-Trimethoxy-3′-aminostilbene disrupts tumor vascular perfusion without damaging normal organ perfusion

David Durrant · Frank Corwin · Daniele Simoni · Ming Zhao · Michelle A. Rudek · Fadi N. Salloum · Rakesh C. Kukreja · Panos P. Fatouros · Ray M. Lee

Received: 14 December 2007 / Accepted: 28 February 2008 / Published online: 26 March 2008

Abstract
Purpose Targeting tumor vasculature by colchicine site microtubule inhibitors is a new approach in cancer therapy. Here we investigate *cis*-3, 4′, 5-trimethoxy-3′-aminostilbene (stilbene 5c) in its effect on tumor vascular perfusion, pharmacokinetics, toxicity and therapeutic efficacy in a mouse xenograft model.
Methods Tumor xenograft model was established with subcutaneous injection of UCI-101 ovarian cancer cells into nude mice. Tumor blood perfusion was investigated by dynamic contrast-enhanced (DCE) MRI studies. Pharmacokinetic studies were performed by LC/MS/MS to quantify the concentrations of stilbene 5c in plasma. Tumor size was measured by the long and short axes of tumor to calculate tumor volume. Mouse cardiac function study was determined by Doppler echocardiography using the Vevo770TM imaging system. Microvascular density was determined by CD34 staining of tissue sections.
Results Stilbene 5c selectively suppresses tumor perfusion without damaging normal organ perfusion in DCE-MRI studies. Histological sections of normal organs treated with stilbene 5c do not reveal any major toxicity in H&E staining. Microvascular density determined by CD34 staining is unchanged in normal organs, but significantly decreased in tumor after stilbene 5c treatment. Biodistribution study shows that stilbene 5c is not detectable in heart and lung, rapidly decreased in brain, liver, and kidney, but remains high in tumor for more than 3 h after IV injection of stilbene 5c, suggesting preferential accumulation in tumor. Mice treated with 5 days of stilbene 5c had negligible cardiac toxicity based on their normal left ventricular ejection fraction. In vivo efficacy study of stilbene 5c showed that it only suppresses tumor growth by 40% if used alone, but combination with bevacizumab is significantly better.
Conclusion Stilbene 5c is a useful vascular disrupting agent and combination with bevacizumab could be a promising therapy for cancer.

Keywords Stilbenes · Tumor perfusion · Endothelial cells · Bevacizumab · DCE-MRI

D. Durrant · F. N. Salloum · R. C. Kukreja · R. M. Lee (✉)
Department of Internal Medicine, Massey Cancer Center, Virginia Commonwealth University, 1101 E. Marshall Street, Richmond, VA 23298, USA
e-mail: rlee5@vcu.edu

F. Corwin · P. P. Fatouros
Department of Radiology, Massey Cancer Center, Virginia Commonwealth University, Richmond, VA, USA

D. Simoni
Dipartimento di Scienze, Farmaceutiche, Universita di Ferrara, Ferrara, Italy

M. Zhao · M. A. Rudek
Sidney Kimmel Comprehensive Cancer Center, The Johns Hopkins University, Baltimore, MD, USA

Introduction

Tumor growth requires the development of a network of neovasculature to supply oxygen and nutrients and to remove toxic metabolites. The neovasculature formed in the tumor tissue differs significantly from the normal vasculature [1, 2]. Tumor neovasculature is abnormal, chaotic and inadequate in structure and function [3]. Targeting tumor vasculature has evolved into a useful strategy to develop new cancer therapeutics [4]. Two approaches have

been used nowadays to target tumor vessels. One is to prevent the angiogenic process by blocking angiogenic factors or their receptors to prevent the growth of new vessels. The other strategy is to kill the existing endothelial cells in tumor directly. This group of compounds was named as vascular disrupting agents (VDAs). Their goal is to kill tumor endothelial cells and to prevent tumor from getting adequate blood supply, which leads to tumor ischemia and eventually necrosis [5, 6]. A group of colchicine site inhibitors, including combretastatin A4 (CA4), ZD6126, AVE8062 and Oxi4503, kill tumor endothelial cells by interfering with microtubule polymerization. They are effective for anti-vascular purpose in doses that are equivalent to one tenth of their maximally tolerated dose in contrast to vinca alkaloids, which have anti-vascular effect only until reaching maximally tolerated doses. Other small molecules, such as flavonoid DMXAA, induce local release of TNFα or other cytokines from activated macrophages in the tumor tissue to damage tumor vessels [5, 6].

Although direct disruption of tumor vasculature is a promising concept, the caveat of VDAs is the possibility of damaging normal vascular endothelium as shown in the phase I clinical trials for ZD6126 and CA4P, the water-soluble prodrug of CA4 [7–10]. Neither of them induces common side effects of existing chemotherapy such as alopecia and bone marrow toxicity. Three main side effects were observed for CA4P. One is cardiovascular toxicity, including tachycardia, bradycardia, hypertension, and prolongation of QT_c interval. The second is pain in the tumor region. The third is neurological symptoms such as neuropathy, ataxia, headache, and abdominal pain. Cardiovascular and neurotoxicity were considered the dose limiting toxicity [7, 9]. Other non-specific symptoms such as abdominal pain, could also be related to non-specific damage to endothelium of splanchnic circulation, raising a question about the specificity of these VDAs. It was encouraging that a patient with anaplastic thyroid carcinoma achieved complete remission that lasted 30 months, raising a significant interest in subsequent studies on this cancer. Pharmacodynamically, both the agents were capable of suppressing tumor vascular perfusion using PET scan or DCE-MRI studies [7, 11]. In contrast to CA4P, ZD6126 had no neurotoxicity observed, but cardiovascular toxicity appeared to be worse. Decreased left ventricular ejection fraction, elevation of CK and CK-MB, and EKG changes characteristic of acute myocardiac infarction were reported. Circulating endothelial cells increased by 40–60% at 2–8 h after infusion but this increase did not correlate with peak plasma concentrations or drug exposure [10]. The increase of circulating endothelial cells could be a potential issue, since recruitment of endothelial progenitor cells to tumor was detected after treatment of tumor-bearing mice with VDAs [12]. This may lead to revascularization in tumor after drug administration and treatment failure.

Considering these main obstacles of CA4P and ZD6126, it would be necessary to develop other compounds that have more specificity to tumor endothelial cells than normal endothelial cells to avoid the cardiac toxicity. We studied a stilbene derivative, *cis*-3, 4′, 5-trimethoxy-3′-aminostilbene (stilbene 5c), which is also a colchicine site inhibitor of microtubule. This compound has structure similarity to CA4 but does not have a trimethoxylphenyl moiety due to absence of the 4-methoxyl group and substitution of the hydroxyl group of CA4 with an amino group [13] (Fig. 1). Stilbene 5c is highly potent against various tumor cells and blocks cell cycle progression in G_2–M phase. Stilbene 5c is tolerated in mice up to 100 mg/kg and no major organ toxicity was observed [5]. In particular, there was no bone marrow toxicity, and the ability of bone marrow engraftment was not affected by stilbene 5c treatment. Here we describe that stilbene 5c is highly effective in suppressing tumor vascular perfusion without damaging normal organ perfusion in a solid tumor model. Most importantly, the compound has an undetectable level in heart and does not affect mouse cardiac function, suggesting that it could be a more desirable VDA with negligible cardiac toxicity.

Methods

Tumor xenograft model

UCI-101/luciferase ovarian cells were used to generate tumor xenografts in nude mice. Cells were grown in Iscove's Modified Dulbecco's medium (IMDM) supplemented with 10% fetal bovine serum and glutamine/penicillium/streptomycin. Each mouse was injected with 5×10^6 cells intraperitoneally or subcutaneously in back to grow tumor xenografts. Mice were treated with stilbene 5c or 6c (*cis*-3, 4′, 5-trimethoxy-3′-hydroxylstilbene) at 25 mg/kg by intraperitoneal injection. Stilbene 5c and 6c were synthesized as described [13]. Tumor volume was calculated by $ab^2/2$ where "a" and "b" are the long and short axes of tumor.

Effect of stilbenes in human umbilical vein endothelial cells (HUVECs)

HUVECs and their culture media were purchased from Cambrex Corp. (East Rutherford, NJ, USA). Cells were treated with various concentrations of stilbene 5c or 6c before harvested for propidium iodide (PI) staining and FAScan analysis. Alternatively cells were fixed with 2% paraformaldehyde followed by immunofluorescent staining with anti-tubulin antibody. Nuclei were stained with DAPI.

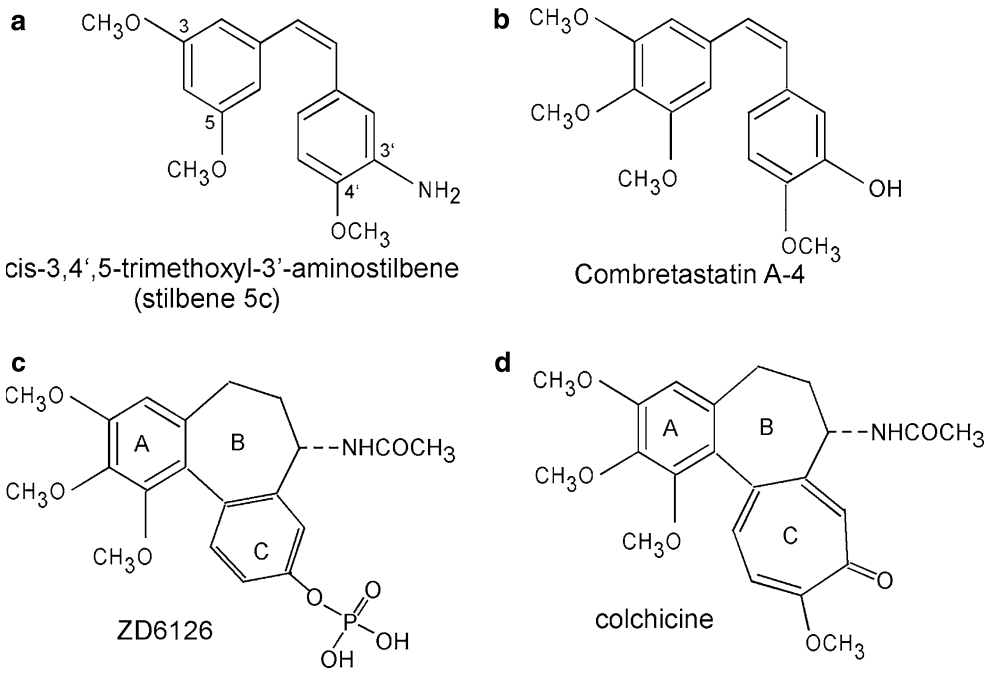

Fig. 1 Chemical structures of stilbene 5c, combretastatin A4, ZD6126 and colchicine. Stilbene 6c is another derivative that replaces the amino group of stilbene 5c with a hydroxyl group and similar to CA4. CA4P has a phosphate group attached to the hydroxyl group of CA4

Determination of tumor and normal organ perfusion by DCE-MRI

Nude mice with tumor xenograft were anesthetized with 1% isoflurane and mixed oxygen. DEC-MRI was performed with experimental MR system (Bruker, Biospec 2.35T/40 cm) that is dedicated to small animal imaging. Jugular vein was dissected to place an IV catheter for contrast injection in acute phase study. The first batch of mice were injected with 50 μL of gadolinium (OmniScan) through the jugular catheter and MRI images were collected every second to investigate the initial rate of increase of MRI signals immediately after injection. After the initial rate is established, subsequent MRI studies focused on the sustained increase in gadolinium signals, which also provide qualitative and quantitative information for tissue perfusion. For this study, 20 μL of gadolinium was injected directly into tail veins. Mice were transferred into the tunnel of MRI machine within 1 min after injection. MRI images were collected every minute for 30 min.

Pharmacokinetic study

For plasma pharmacokinetic studies, BALB/c mice were injected with stilbene 5c at 10 mg/kg intravenously. For tissue distribution study, nude mice with tumor xenografts were injected with stilbene 5c at 20 mg/kg IV. Mice were humanely killed, and plasma and tissues were harvested as a function of time after administration. Blood samples were collected and centrifuged at 3,000 rpm at 4°C for 5 min to obtain plasma. Major organs are dissected and about 100 mg of each organ was extracted for determination of stilbene 5c concentrations. Plasma and tissue samples were frozen at −80°C until LC/MS/MS analysis.

Briefly, stilbene 5c was extracted by acetonitrile containing temazepam as an internal standard. Tissue homogenates were prepared at a concentration of 200 mg/mL in PBS and further diluted 1:10 in human plasma before extraction using acetonitrile. The analytes were separated on a Waters (Milford, MA, USA) X-Terra MS C18 (50 × 2.1 mm, 3.5 μm) column with acetonitrile containing 0.1% formic acid/10 mM ammonium acetate mobile phase (70:30, v/v) using isocratic flow at 0.15 mL/min for 5 min. Stilbene 5c was monitored by tandem-mass spectrometry with electrospray positive ionization. Calibration curves were generated over the range of 0.005–1 μg/mL for plasma and 0.3–60 μg/g for tissue. Samples that were above the limits of quantitation were diluted with plasma prior to analysis.

Pharmacokinetic variables were calculated from mean stilbene 5c concentration–time data using non-compartmental methods as implemented in WinNonlin version 5.0 (Pharsight Corp., Mountain View, CA, USA) [14]. C_{max} was the observed values from the mean data. The AUC up to 4 h was calculated using the linear trapezoidal method. The AUC values were extrapolated to infinity (AUC_{inf}) by dividing the last quantifiable concentration by the terminal disposition rate constant (λ_z), which was determined from the slope of the terminal phase of the concentration–time

profile. The terminal half-life ($t_{1/2}$) was calculated as 0.693 divided by λ_z. The clearance (Cl) was calculated by dividing the dose administered by AUC_{inf}.

Immunohistochemistry study of tissue sections

After mice were sacrificed, major organs and tumors were dissected and fixed in 10% formalin. Tissues were embedded in paraffin and sections were stained with H&E, and with antibody against CD34 for quantification of microvascular density. The scoring of microvascular density was based on the methods described by Weidner et al. [15, 16] by counting the CD34-positive signals in a photo frame of 200× magnification using Nikon ECLIPSE E800M microscope equipped with a Diagnostic Instruments Spot RT CCD camera.

Doppler echocardiography

Doppler echocardiography was performed using the Vevo770TM imaging system (VisualSonics Inc., Toronto, Ontario, Canada) prior to treatment with stilbene 5c, and 4 h and 7 days after treatment. Light anesthesia was used during the exam with the injection of pentobarbital (30 mg/kg; ip). The mice were placed in the supine position and ECG limb electrodes were attached. The chest was carefully shaved and ultrasound gel was used on the thorax to optimize visibility during the exam. A 30-MHz probe was utilized to obtain two-dimensional, M-mode and Doppler imaging from parasternal short-axis view at the level of the papillary muscles and the apical four-chamber view [17]. M-mode images of the LV were obtained and systolic and diastolic wall thickness (anterior and posterior) and LV end-systolic and end-diastolic diameters (LVESD and LVEDD, respectively) were measured. LV fractional shortening (FS) was calculated as (LVEDD − LVESD)/LVEDD × 100. Ejection fraction was calculated using the Teichholz formula [18]. The LV mass was calculated using the following formula (LVEDD + AWDT + PWDT)3 − (LVEDD)3 × 0.8 × 1.04) + 0.6)/1,000, where AWDT and PWDT are anterior and posterior wall diastolic thickness, respectively [19]. The allocation to different treatments was random, and the investigators performing and reading the echocardiogram were blinded to the treatment.

Results

Stilbenes 5c and 6c induce human umbilical vein endothelial cell apoptosis

To investigate whether stilbenes are capable of damaging tumor endothelial cells similar to CA4, we first tested their sensitivity in commercially available HUVECs. HUVECs were cultured with stilbene 5c for 16 h and stained with PI for cell cycle analysis. Cell cycle arrest at G_2 and appearance of a large $subG_{0/1}$ population of population were observed when HUVECs were treated with 30 nM stilbene 5c overnight (Fig. 2a). Immunofluorescent staining of tubulin showed disruption of microtubules when HUVECs were treated with 30 and 100 nM stilbene 5c or 100 nM stilbene 6c (Fig. 2b). DAPI staining revealed the appearance of nuclear condensation and fragmentation that represent apoptosis.

Stilbene 5c selectively disrupts tumor vascular perfusion

Next we studied the vascular disrupting effect of stilbene 5c in vivo using DCE-MRI to measure vascular perfusion of tumor before and after stilbene treatment. We first focused on the early phase within the first minute after injection of gadolinium to study the dynamics of tumor perfusion. Catheters were placed in the jugular vein and gadolinium

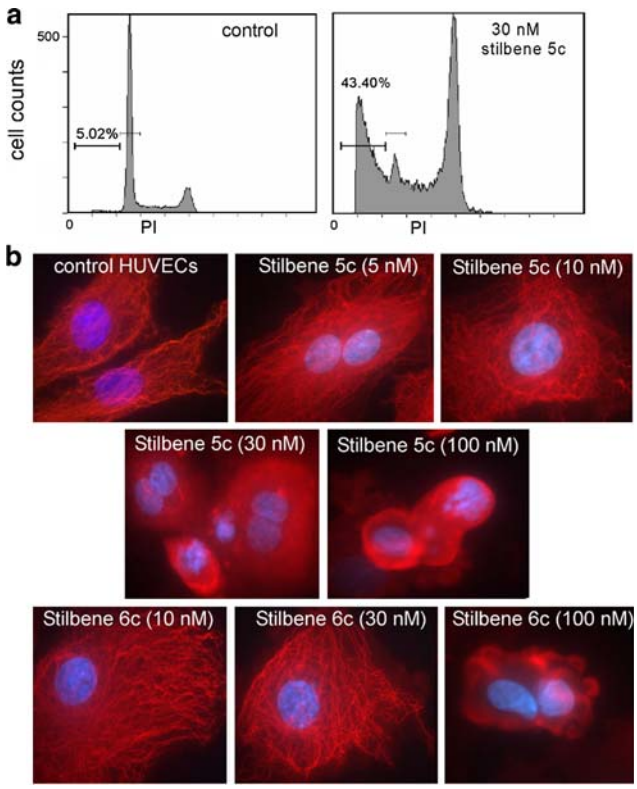

Fig. 2 HUVECs are highly sensitive to stilbenes 5c and 6c. **a** Flow cytometry analysis. HUVECs were incubated with stilbene 5c overnight and harvested for PI staining followed by flow cytometry analysis. The sub-G_1 population represents the dead cells. **b** Disruption of microtubule and induction of apoptosis by stilbenes 5c and 6c. HUVECs were treated with stilbenes 5c and 6c for 16 h and fixed with paraformaldehyde followed by immunofluorescent staining with anti-tubulin antibody. Tubulin in *red* and nuclei are stained with DAPI in *blue*

contrast was injected through the catheter. After MRI images were collected every second for 10 min, the initial rising slopes were calculated in tumor and compared with paraspinal muscle, which was used as normal tissue control. In three untreated mice, the muscle had a rate of rise at 903, 1320, and 886/s, and the corresponding tumor in the same mice has a rate at 219, 552, and 319/s, respectively (24.3, 41.8 and 36.0% of muscle, respectively). The average ratio of tumor blood flow is $34.0 \pm 8.9\%$ of that of muscle. At 4 h after stilbene 5c treatment, the rate in muscle was unchanged at 985, 1354, and 921/s, respectively in those three mice. In contrast, that of the corresponding tumor decreased to 135, 383, and 254/s (13.7, 28.3 and 27.5% of muscle, respectively). The average ratio of tumor blood flow decreases to $23.2 \pm 8.2\%$ of that of muscle in three stilbene 5c-treated mice (Fig. 3), which is statistically significant compared with untreated mice. There was a 32% drop in the rate of initial tumor perfusion relative to muscle at 4 h after stilbene treatment.

Considering the unpredictable nature of tumor perfusion regarding time and spatial variations, we also studied the later phase of gadolinium entry into tumor. The previous rapid kinetic studies showed that after 10 min of rapid increase the gadolinium signals reached plateau and persisted for at least 30 min without washing out. We chose 30 min after injection for studying the images in plateau. In addition, using tail vein injection rather than a surgery to place jugular vein catheter, we were able to compare same mice before and after stilbene treatment to avoid individual variation in mice. Mice were first imaged without contrast to obtain a baseline (Fig. 4a, left upper panel). The section was obtained at the center of the tumor. Kidney, which has a better late enhancement, in the same section was used as an internal organ control. After injected with 20 μL of gadolinium (OmniScan) via the tail vein, mice were analyzed with a rapid sequence MRI every minute for total of 30 min. Both the tumor and kidney exhibited enhancement of MRI signals after injection of gadolinium, which represented vascular perfusion of tumor and kidney (Fig. 4a, right upper panel). Mice were then left for 24 h to let gadolinium washed out. Same mice were treated with 50 mg/kg stilbene 5c by intraperitoneal injection on the second or third day. Four hours after injection of stilbene 5c, mice were imaged again before and after gadolinium injection by the same protocol and compared with the previous pair of images before stilbene treatment. In the baseline image before gadolinium injection, the T1-weighted image had a slight increase of MRI signals (Fig. 4a, left lower panel) compared with the baseline image of untreated mice. This increased signal was likely due to a small amount of residual gadolinium left in the body from the previous day. After injection of gadolinium, kidney and other normal organs showed enhanced signals. However, the tumor region showed significantly less gadolinium enhancement compared with that before stilbene treatment (Fig. 4a, right panels), suggesting that stilbene 5c selectively inhibits tumor perfusion and spares normal organs. Similar studies were performed in six mice and the T1 map was generated for each mouse. The concentration of gadolinium was calculated from each image and results are shown in Fig. 4b. The algorithm of calculation failed in kidney due to the fact that the signals in kidney reached saturation. The concentration of gadolinium in tumor decreased to an average of 62.8% in tumor at 4 h after stilbene treatment. In contrast, the concentration of gadolinium in muscle did not change with stilbene treatment, indicating that stilbene 5c selectively suppresses tumor perfusion without compromising normal vascular perfusion.

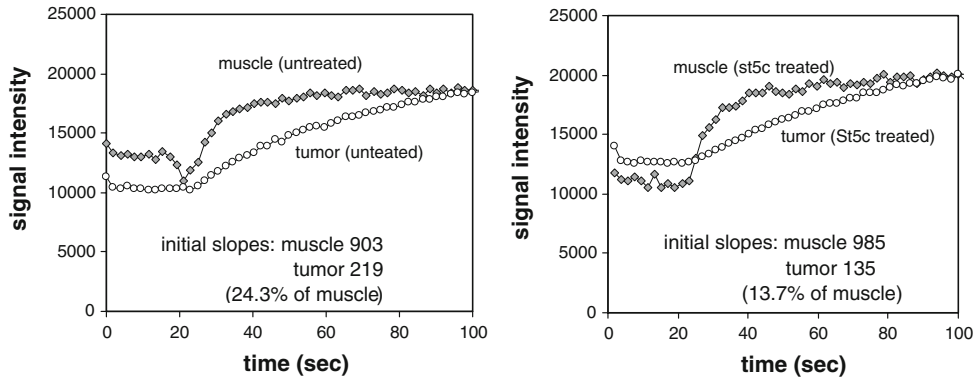

Fig. 3 Initial accumulation of gadolinium in tumor in a DCE-MRI study. Nude mice with established subcutaneously UCI101 tumor xenografts were analyzed with DCE-MRI for tumor perfusion. Catheters were placed in the jugular vein for IV injection of gadolinium. MRI sections were collected every second immediately after bolus injection of 50 μL of gadolinium (OmniScan). The MRI signal intensity of the region of interest was plotted against time in the first 100 s. The initial slopes of the first 2 s were calculated in muscle and tumor to represent the rate in gadolinium accumulation and listed in the figures. Shown are the representatives of three untreated and three treated mice

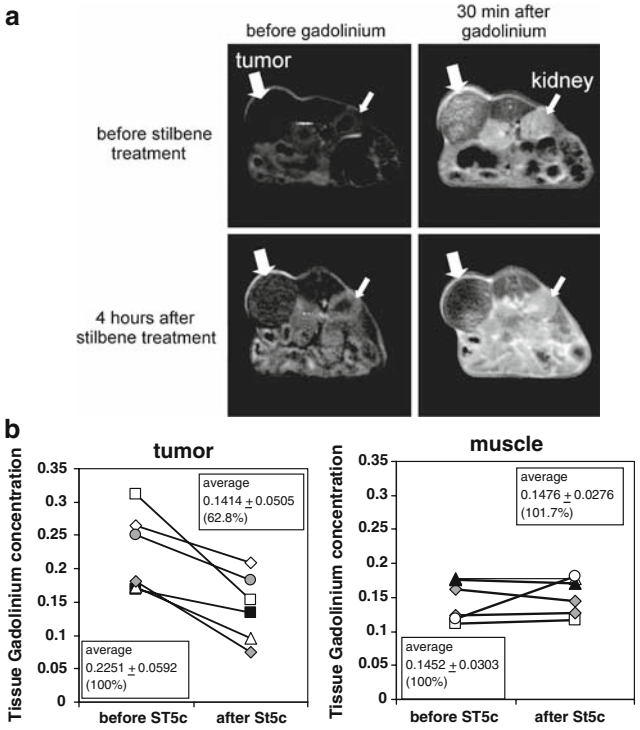

Fig. 4 Study of tumor perfusion using accumulation of gadolinium at 30 min after gadolinium injection. **a** T1-weighted images before and after stilbene 5c treatment in the same mouse. Nude mice with established subcutaneously UCI101 tumor xenografts were analyzed with DCE-MRI for tumor perfusion. DCE-MRI images were collected for 30 min after injection of OmniScan into tail veins. Same mice were studied before and after stilbene 5c treatment to avoid individual variation. Left panels showed the T1-weighted images before injection of gadolinium. Right panels showed images at 30 min after injection of gadolinium. The upper panels showed gadolinium enhancement in tumor and kidney before mice were treated with stilbene 5c. The *lower panels* showed kidney enhancement remained the same similar to the condition before stilbene treatment. However, stilbene 5c treatment dramatically decreased tumor enhancement by gadolinium (*right lower panel*) compared with the right upper panel before stilbene treatment. Tumor is marked with *big arrowhead* and kidney with *small arrowhead* in each image. Shown are the representative images of one of six mice that were studied. **b** Average of calculated gadolinium concentrations in tumor and muscle before and after stilbene 5c treatment. Same experiments were performed in six mice for statistical analysis. For calculation of tissue gadolinium concentration to represent the tissue perfusion, T1 map before and 30 min after gadolinium injection was generated. Tumors signals decreased to 62.8% in average after stilbene 5c treatment; whereas muscle shows no significant change after stilbene treatment

Stilbene 5c is preferentially accumulated in tumor but not in heart, lung or spleen

Mice were injected with stilbene 5c at 10 mg/kg intravenously to determine the pharmacokinetics. Our study revealed that stilbene 5c has an average half-life of 1.8 h, $AUC_{0-4\,h}$ 143 h × ng/mL, AUC_{inf} 1,524 h × ng/mL, C_{max} 2,302 ng/mL and clearance 32.9 L/h.

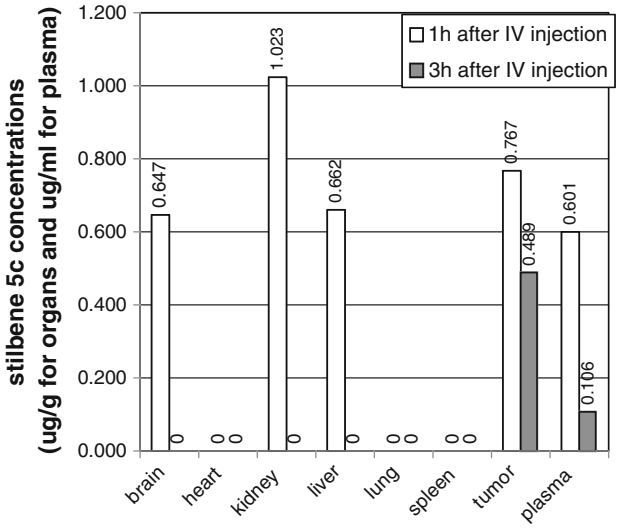

Fig. 5 Biodistribution of stilbene 5c after intravenous injection. Nude mice with established UCI101 tumor xenografts were treated with stilbene 5c at 20 mg/kg and mice were sacrificed at 1 and 3 h after injection. Various organs and tumor were harvested for extraction for the determination of stilbene 5c concentrations by LC/MS/MS. The drug concentration was normalized by the tissue weight. Two mice were studied in each time point and the results are the averages of two mice. The average concentrations are labeled at the top of each *bar* in histogram

We then investigated the biodistribution of stilbene 5c in normal organs and tumor xenografts. Plasma, tumors and various organs including brain, heart, lung, liver, kidney and spleen were harvested for extraction and the concentrations of stilbene 5c in each organ was determined. Stilbene 5c was not detected in heart, lung and spleen at either 1 or 3 h after intravenous injection (Fig. 5), but was present in brain, kidney and liver at 1 h after injection of stilbene 5c at a level comparable to that in plasma. Subsequently, the levels in these three organs decreased to undetectable level at 3 h after injection. In contrast, the level of stilbene 5c in tumor xenograft remained persistently high at 3 h (63% of that at 1 h, Fig. 5). This finding indicates that stilbene 5c is preferentially accumulated in the tumor xenograft.

Immunohistochemistry staining with CD34 vascular marker in sections of tumor and normal organs

We took tissues that were studied with DCE-MRI to investigate the vascular density of tumor and correlate with the results from DCE-MRI-derived vascular perfusion studies. We particularly examined sections from heart and brain, where the toxicity of colchicine site inhibitors was observed. Tissue sections were stained with standard H&E and anti-CD34 (an endothelial marker) antibody by immunohistochemistry staining. The H&E staining did not show any significant changes in any

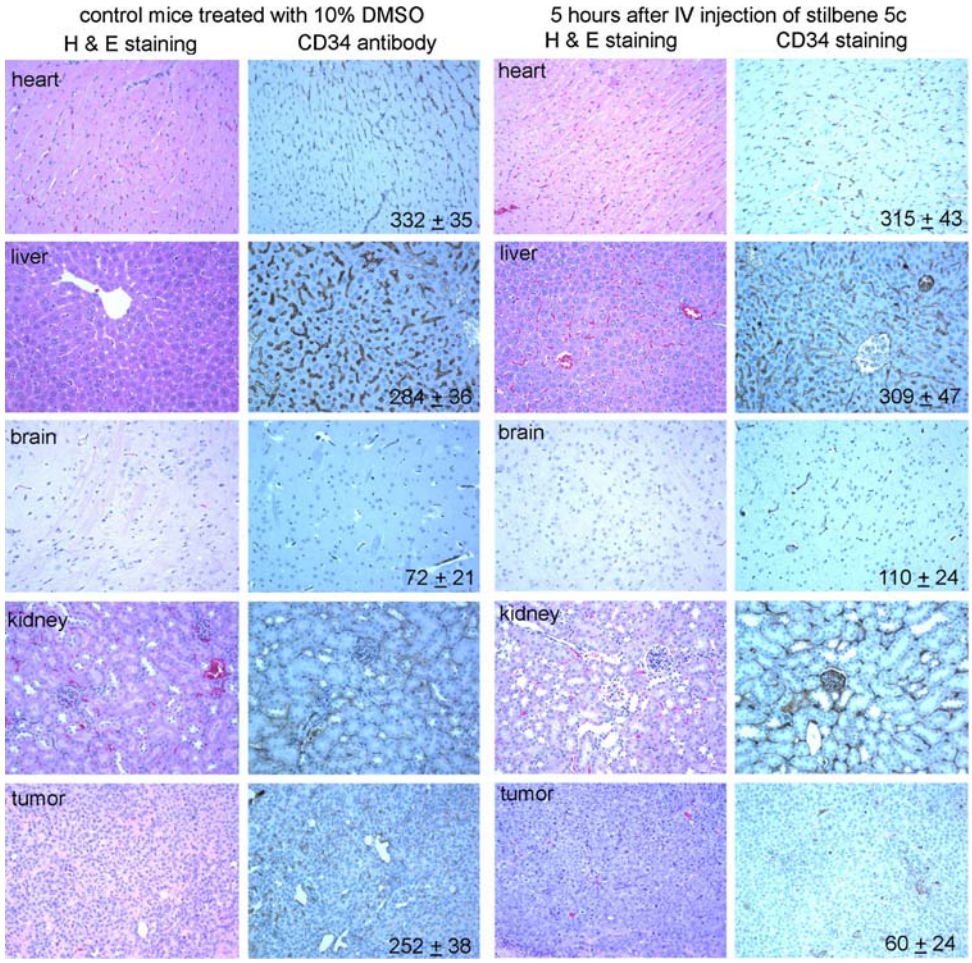

Fig. 6 Stilbene 5c treatment decreases microvascular density in tumor but not in normal organs. Nude mice with UCI tumor xenograft were treated with 10% DMSO or stilbene 5c at 50 mg/kg intraperitoneally. Mice were sacrificed at 4 h after injection, and various organs and tumor were harvested for fixation and standard H&E staining. Immunohistochemical staining of each section was performed with anti-CD34 antibody to quantify the microvascular density. The *brown color* in each immunohistochemical stained section is the positive signal for CD34 staining. Shown are the pictures in ×200 fold magnification. The numbers of positive signals in each CD34 stained picture are counted and are shown in the right lower corner of each panel. Shown are the averages and standard deviations of four different fields that show the most abundant microvascular density. The sections from kidney cannot be scored due to the fact that all vessels around renal tubules are fused into a large network in the picture. These results suggest that tumor vascular density was dramatically decreased by nearly four folds, whereas that of other organs, heart, liver, brain and kidney was not affected by stilbene 5c treatment

major organs after stilbene 5c treatment (Fig. 6). There was also no histological difference in tumor either. We then used anti-CD34 staining to score microvascular density in tumor and various normal organs [15, 16]. The results are indicated at the right lower corner of each panel except kidney, which cannot be scored due to fusion of the capillary network rather than discrete dots or tubes in appearance. Treatment with stilbene 5c does not change the microvascular density of heart, liver, kidney and brain, but significantly decrease that of tumor to nearly one fourth (Fig. 6). This finding is consistent with our MRI result that stilbene 5c selectively decreased tumor vascular perfusion without compromising normal organ perfusion.

Stilbene 5c does not compromise cardiac function

The major concern for VDAs such as CA4 and ZD6126 is their cardiac toxicity in the phase I clinical trials [7, 9, 10]. As cardiac toxicity is a serious side effect, we perform further cardiac function study to rule out the possibility that stilbene 5c may exhibit cardiac toxicity even though there was minimal stilbene 5c accumulated in heart and histological section of the heart was normal in mice treated with stilbene 5c. Echocardiogram was used to study the heart chamber size and ejection fraction of mice before and after they were treated with stilbene 5c ($n = 7$). After establishment of baseline for each mouse, echocardiogram was repeated at 4 h after 25 mg/kg stilbene 5c treatment and at

day 7 after mice were treated daily in days 1–5. All the parameters we measured, including systolic and diastolic chamber sizes, anterior and posterior wall thickness, fractional shortening and ejection fraction of the left ventricle all remained the same in all three analyses, indicating that the cardiac function of mice was not affected either acutely after 4 h or chronically after 5 days of stilbene treatment (Table 1).

Efficacy of stilbene 5c in tumor growth in mouse xenograft models

Next we used ovarian cancer UCI101 cells to study the in vivo efficacy of stilbene 5c. We first administered stilbene 5c with intraperitoneal injection at 25 mg/kg three times a week. Tumor volume was calculated by measuring the long and short axes. Unfortunately, we did not detect any difference in tumor growth between control and stilbene 5c-treated mice (not shown). The result that stilbene 5c is not effective as a single agent is not a surprise based on what is known for CA4. CA4 by itself as single agent also failed to show tumor growth suppression [20–22]. This is thought to be due to the viable tumor rim, which survives the treatment with VDAs by getting nutritional and blood support from surrounding normal vasculature. When treatment with VDAs is stopped, the viable rim of surviving tumor grows quickly. Tumor vasculature recovers quickly by recruitment of the mobilized endothelial progenitor cells [12]. Based on this rationale, we combined stilbene 5c with bevacizumab, which was used to neutralize VEGF secreted by UCI-101 tumor cells. To achieve a better therapeutic efficacy, we increase the frequency of stilbene 5c treatment to five consecutive days (Monday–Friday) for 2 weeks at 20 mg/kg/day since the half-life of stilbene 5c is 1.8 h. Bevacizumab was given at 10 mg/kg twice a week (Mondays and Fridays) for five doses. The group treated with stilbene 5c alone had tumor growth suppression about 45%, and the group treated with bevacizumab alone had tumor growth suppression at about 25%. The group treated with combination of stilbene 5c and bevacizumab achieved 80% tumor growth suppression (Fig. 7). After dissecting of the tumor at 24 days. The weight of the tumor confirmed the measurement result (not shown). This study leads to two conclusions. Stilbene 5c is more effective if given more frequently and stilbene 5c is much more effective when combined with angiogenic inhibitor bevacizumab.

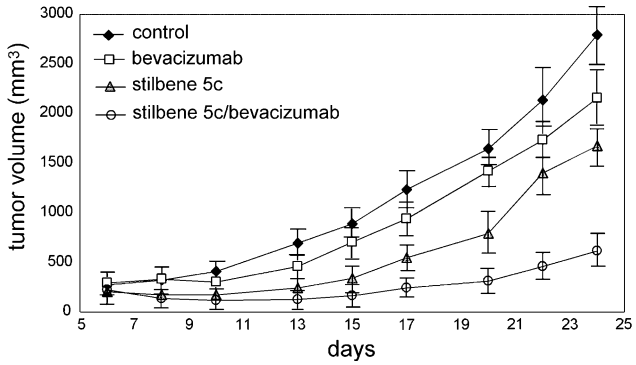

Fig. 7 Stilbene 5c can enhance the effect of bevacizumab in vivo. Nude mice were injected with UCI-101 cells subcutaneously and mice are treated with stilbene 5c at 20 mg/kg/day Monday–Friday with or without bevacizumab 10 mg/kg twice a week. Tumor volume was calculated by the long and short axes. Each group contains eight mice and the average tumor volumes and standard deviations were plotted against days

Discussion

Targeting tumor vasculature has evolved into a promising strategy for cancer therapy. The anti-angiogenic approach has been well established with the success of anti-VEGF antibody bevacizumab and VEGF receptor tyrosine kinase inhibitors sorafenib and sunitinib in various cancers [23, 24]. The more direct endothelial targeting VDAs are still in developing now. VDAs of the first generation, including CA4P and ZD6126, were noted to have cardiac toxicity in phase I clinical trials [7, 9, 10]. Other tyrosine kinase inhibitors were also reported to have cardiac toxicity [25]. Since these agents have high potency against vascular endothelial cells, damaging normal vascular endothelium could potentially lead to vascular occlusion, myocardiac ischemia or even infarction or ischemic stroke in brain. Compounds of

Table 1 Parameters of echocardiogram in mice before treatment and treated with stilbene 5c at 4h and 7 days (5 daily dosing)

	Baseline	4 h after treatment	7 days
End diastolic diameter	3.13 ± 0.44	3.04 ± 0.44	3.26 ± 0.36
End systolic diameter	1.82 ± 0.48	1.59 ± 0.27	1.85 ± 0.23
Anterior wall diastolic thickness	0.93 ± 0.13	0.90 ± 0.19	0.92 ± 0.20
Posterior wall diastolic thickness	0.92 ± 0.14	1.07 ± 0.29	0.99 ± 0.13
Anterior wall systolic thickness	1.32 ± 0.11	1.42 ± 0.24	1.30 ± 0.25
Anterior wall systolic thickness	1.22 ± 0.28	1.42 ± 0.36	1.32 ± 0.23
Fractional shortening	42.87 ± 9.45	47.66 ± 8.15	43.47 ± 1.84
Ejection fraction	73.86 ± 8.17	73.14 ± 6.67	73.71 ± 2.56

the second generation will need to avoid this potential problem and be more specific to tumor endothelial cells. Here we investigate stilbene derivatives, with stilbene 5c as a potent member of the family. We found that stilbene 5c induces cell death in HUVECs. Using DCE-MRI, we demonstrated that stilbene 5c selectively suppressed tumor vascular perfusion without compromising normal organ perfusion. To address the potential problem of cardiovascular toxicity, we investigated drug distribution in various organs. The level of stilbene 5c was undetectable in heart and lung even as early as 1 h after IV injection. This was reflected in the microvascular density study that the patterns of endothelial cells in heart and lung have no acute change in mice treated with stilbene 5c at a dose of 50 mg/kg. Cardiac function study with echocardiogram demonstrated that stilbene 5c does not decrease LV ejection fraction.

The pharmacokinetic profile of stilbene 5c shows an advantage of tumor accumulation. The plasma half-life of stilbene 5c is around 1.8 h in mice. Brain, liver, kidney and tumor were the main organs that have high levels of stilbene 5c at 1 h after IV administration. The level in these three organs decreased rapidly to undetectable at 3 h. In contrast, stilbene level in tumor remains high at the same time point, indicating that the half-life in tumor is much longer than that in normal organs. This preferential tumor accumulation could have a few possibilities, such as preferential accumulation of stilbene 5c in tumor due to the abnormal tumor vasculature or slower in metabolism of stilbene 5c in tumor. Regardless of the etiology, this feature is a desirable characteristic to further develop stilbene 5c. The pharmacokinetic result of stilbene 5c can also be correlated with our DCE-MRI study, which was performed at 4 h after stilbene treatment. This timing is about two serum half-life, in which there is no drug left in normal organs, but stilbene 5c is still present at a sufficient amount in tumor to damage endothelial cells. Our DCE-MRI study did not reveal how soon the tumor blood flow is suppressed after administration of stilbene 5c. However, we believe that this is a fast process since tumor endothelial cells could undergo apoptosis after exposure to stilbene 5c. When endothelial cells are striped off from tumor vessels after apoptosis, blood clotting occurs immediately after the exposed connective tissue, clotting factors and platelets interact. The retained stilbene 5c in tumor tissue will further prevent the recovery of the endothelial cells and continue to suppress tumor perfusion up to 4 h as shown in DCE-MRI studies.

In the tumor xenograft study, stilbene 5c alone did not induce robust tumor growth suppression when it was given by itself. Same scenario has been observed in CA4, and perhaps most of the VDAs, which do not induce significant tumor growth suppression alone. Although it can induce central tumor necrosis, the peripheral tumor can obtain blood perfusion through surrounding normal vessels and escape the effect of vascular disrupting agent. When drug administration is stopped, the viable rim will grow back and compromise the efficacy of tumor growth suppression. The recent report by Shaked et al. [12], that tumor recruits circulating endothelial progenitor cells after CA4 treatment, provides another mechanism why VDAs may not work by itself. One way to solve this problem is by prolongation of drug administration, as shown by the better efficacy if given daily. The second approach is by combination with anti-angiogenic agents. After VDAs shut down tumor vascular perfusion, tumor becomes hypoxia and commits necrosis. During this course, tumor responds to hypoxia by producing angiogenic factors to mobilize endothelial progenitor cells, which will be recruited to tumor bed and re-establish tumor vasculature. Addition of anti-angiogenic agents such as bevacizumab, which is shown to prevent mobilization of endothelial progenitor cells [26] and block VEGF-induced endothelial proliferation, will be expected to have a synergistic effect with VDAs. Our combination study in Fig. 7 proved this concept.

In conclusion, we have demonstrated that stilbene 5c is a potent VDA that selectively suppresses tumor vascular perfusion. Combination with an anti-angiogenic agent will be essential to achieve the best in vivo efficacy for stilbene 5c. Its toxicity profile suggests that stilbene 5c has negligible cardiac toxicity but it remains to be determined if this will prove to be a clinical advantage when the drug is evaluated in patients.

Acknowledgments This study was supported by Massey Cancer Center pilot funding (R.M.L.) and in part by grants from National Institutes of Health to R.C.K. (HL51045, HL59469, and HL79424). We thank Dr. Zhijian Chen for technical assistance in placing jugular catheters. Microscopy was performed at the VCU—Department of Neurobiology and Anatomy Microscopy Facility, supported, in part, with funding from NIH-NINDS Center core grant (5P30NS047463).

References

1. Eberhard A et al (2000) Heterogeneity of angiogenesis and blood vessel maturation in human tumors: implications for antiangiogenic tumor therapies. Cancer Res 60(5):1388–1393
2. McDonald DM, Choyke PL (2003) Imaging of angiogenesis: from microscope to clinic. Nat Med 9(6):713–725
3. Carmeliet P, Jain RK (2000) Angiogenesis in cancer and other diseases. Nature 407(6801):249–257
4. Bikfalvi A, Bicknell R (2002) Recent advances in angiogenesis, anti-angiogenesis and vascular targeting. Trends Pharmacol Sci 23(12):576–582
5. Neri D, Bicknell R (2005) Tumour vascular targeting. Nat Rev Cancer 5(6):436–446
6. Tozer GM, Kanthou C, Baguley BC (2005) Disrupting tumour blood vessels. Nat Rev Cancer 5(6):423–435
7. Stevenson JP et al (2003) Phase I trial of the antivascular agent combretastatin A4 phosphate on a 5-day schedule to patients with cancer: magnetic resonance imaging evidence for altered tumor blood flow. J Clin Oncol 21(23):4428–4438

8. Cooney MM et al (2004) Cardiovascular safety profile of combretastatin a4 phosphate in a single-dose phase I study in patients with advanced cancer. Clin Cancer Res 10(1 Pt 1):96–100
9. Rustin GJ et al (2003) Phase I clinical trial of weekly combretastatin A4 phosphate: clinical and pharmacokinetic results. J Clin Oncol 21(15):2815–2822
10. Beerepoot LV et al (2006) Phase I clinical evaluation of weekly administration of the novel vascular-targeting agent, ZD6126, in patients with solid tumors. J Clin Oncol 24(10):1491–1498
11. Anderson HL et al (2003) Assessment of pharmacodynamic vascular response in a phase I trial of combretastatin A4 phosphate. J Clin Oncol 21(15):2823–2830
12. Shaked Y et al (2006) Therapy-induced acute recruitment of circulating endothelial progenitor cells to tumors. Science 313(5794):1785–1787
13. Roberti M et al (2003) Synthesis and biological evaluation of resveratrol and analogues as apoptosis-inducing agents. J Med Chem 46(16):3546–3554
14. Bailer AJ (1988) Testing for the equality of area under the curves when using destructive measurement techniques. J Pharmacokinet Biopharm 16(3):303–309
15. Weidner N et al (1991) Tumor angiogenesis and metastasis—correlation in invasive breast carcinoma. N Engl J Med 324(1):1–8
16. Weidner N et al (1992) Tumor angiogenesis: a new significant and independent prognostic indicator in early-stage breast carcinoma. J Natl Cancer Inst 84(24):1875–1887
17. Schiller NB et al (1989) Recommendations for quantitation of the left ventricle by two-dimensional echocardiography. American Society of Echocardiography Committee on Standards, Subcommittee on Quantitation of Two-Dimensional Echocardiograms. J Am Soc Echocardiogr 2(5):358–367
18. Teichholz LE et al (1976) Problems in echocardiographic volume determinations: echocardiographic–angiographic correlations in the presence of absence of asynergy. Am J Cardiol 37(1):7–11
19. Devereux RB et al (1986) Echocardiographic assessment of left ventricular hypertrophy: comparison to necropsy findings. Am J Cardiol 57(6):450–458
20. Pettit GR et al (1989) Isolation and structure of the strong cell growth and tubulin inhibitor combretastatin A-4. Experientia 45(2):209–211
21. Dorr RT et al (1996) Antitumor activity of combretastatin-A4 phosphate, a natural product tubulin inhibitor. Invest New Drugs 14(2):131–137
22. Dark GG et al (1997) Combretastatin A-4, an agent that displays potent and selective toxicity toward tumor vasculature. Cancer Res 57(10):1829–1834
23. Garcia JA, Rini BI (2007) Recent progress in the management of advanced renal cell carcinoma. CA Cancer J Clin 57(2):112–125
24. Rini BI (2007) Vascular endothelial growth factor-targeted therapy in renal cell carcinoma: current status and future directions. Clin Cancer Res 13(4):1098–1106
25. Force T, Krause DS, Van Etten RA (2007) Molecular mechanisms of cardiotoxicity of tyrosine kinase inhibition. Nat Rev Cancer 7(5):332–344
26. Willett CG et al (2004) Direct evidence that the VEGF-specific antibody bevacizumab has antivascular effects in human rectal cancer. Nat Med 10(2):145–147